

Infrared signatures of positive and negative charge carriers in conjugated polymers with low band gaps

H. Neugebauer *

Linz Institute for Organic Solar Cells (LIOS), Physical Chemistry, Johannes Kepler University Linz, Altenbergerstrasse 69, A-4040 Linz, Austria

Received 14 April 2003; received in revised form 24 July 2003; accepted 21 September 2003

Abstract

The absorption pattern of infrared active vibrations (IRAVs) of p- and n-doped thiophene based conjugated polymers with low electronic band gaps are compared. The polymers were doped electrochemically and studied in situ with attenuated total reflection Fourier transform infrared spectroelectrochemistry. Substantial spectral differences were found for polyethylenedioxythiophene (PEDOT), a polyisothianaphthenemethine derivative (PIM) and two polydithienothiophenes (PDTT1 and PDTT2), whereas PDTT3 has no significant differences in the IRAV spectra. The results are related both to structural effects with selective participation of different chain units (for PIM) and to different localisation of the doping induced charge carriers of both signs (for PEDOT, PDTT1 and PDTT2).

© 2003 Elsevier B.V. All rights reserved.

Keywords: Polythiophenes; p-doping; n-doping; IRAV; Infrared spectroelectrochemistry

1. Introduction

Upon doping, new and very intense infrared active vibration (IRAV) bands appear in the infrared spectra of conjugated polymers due to a strong electron-phonon coupling. In addition, electronic absorption bands at higher energy appear, which are correlated to transitions involving in-the-gap states of charged quasi-particles, usually described as polarons [1]. With amplitude mode (AM) formalism, Horovitz and co-workers presented a model to explain IRAV bands in doped polyacetylene by relating the bands to the influence of the excitation on the single and double bond length alternation along the polymer backbone (“amplitude oscillation”) [2,3]. In the “effective conjugation coordinate” (ECC) theory, Zerbi and co-workers showed the correlation between IRAV bands of conjugated polymers and the IR activation of totally symmetric A_g modes [4,5]. ECC describes the geometrical changes from the ground state to the excited state of the polymer. Ehrenfreund and Vardeny [6] established a link between the electronic ab-

sorption bands and the IRAV bands of doping induced spectra using a model introduced by Girlando et al. (GPS model) [7]. However, all of these theories, developed for relatively simple systems such as polyacetylene and extended to a few polyheteroaromatics, do not account for possible differences in the IRAV signatures of positive and negative charge carriers obtained by p- and n-doping, respectively.

Actually, more complex systems, like thiophene based fused ring polymers, show different behaviour. These systems are promising candidates for applications, since they often have low electronic $\pi \rightarrow \pi^*$ band gaps and unusual optical properties [8,9]. Low band gap materials (band gap smaller than 1.8 eV) are important e.g. for photovoltaic applications [10] since their absorption matches more closely the solar emission spectrum compared with usually used polymers with band gaps larger than 2 eV [11]. To compare the behaviour for both signs of doping in these substances, investigations on doping induced IRAV bands and conclusions to electronic effects by analysing the infrared spectra are necessary. Preferentially these comparative studies should be performed with in situ experiments, where p- and n-doping are carried out in one setup on the same

* Tel.: +43-732-2468-766; fax +43-732-2468-8770.

E-mail address: helmut.neugebauer@jku.at (H. Neugebauer).

sample. Besides photoexcitation (photodoping), doping can be performed either by chemical or electrochemical oxidation (p-doping) or reduction (n-doping). A general and preferential way is by electrochemistry, where the redox processes are determined by the electrode potential. In this way, defined and reproducible doping can be obtained by the control of electrochemical parameters.

Infrared spectroelectrochemical techniques for the study of electrode reactions were introduced more than two decades ago, mostly for the study of the electrochemical behaviour of adsorbed layers [12–14]. A number of modifications and extensions to other systems, e.g. internal reflection spectroscopy of conjugated polymers, have evolved since then [15–17].

In the present paper, the IRAV patterns of thiophene based low band gap conjugated polymers, that undergo both reversible electrochemical p- and n-doping, are compared. Electrochemical doping has been performed with cyclic voltammetric experiments, and infrared spectra were obtained in situ with attenuated total reflection Fourier transform infrared (ATR-FTIR) spectroscopy. The polymers described:

- poly(3,4-ethylenedioxythiophene) (PEDOT),
- a soluble derivative of poly(isothianaphthene methine), poly[(benzo(c)thiophene-1,3-diyl)(p-(hexyloxy)benzylidene) (benzo(c)thiophenequinodimethane-1,3-diyl)] (PIM),
- three members of the family of polydithienothiophenes (PDTTs), poly(dithieno[3,4-b:3,4-d]-thiophene)

(PDTT1), poly-(dithieno[3,4-b:3,2-d]thiophene) (PDTT2), and poly-(dithieno[3,4-b:2,3-d]thiophene) (PDTT3).

The structures of the polymers are shown in Fig. 1. Details of the characterisation of the compounds and their general properties are described in previous publications [18–21].

2. Experimental

For ATR-FTIR spectroscopy, a Bruker IFS66S spectrometer with an MCT detector was used. The spectra were measured with a spectral resolution of 4 cm^{-1} . The setup for ATR-FTIR spectroelectrochemistry is shown in Fig. 2. A slightly n-doped Ge reflection element, for catalytic purposes also covered with a very thin Pt layer, was used as the working electrode and as a waveguide for the IR radiation. The polymer layers were either electropolymerised from monomer solution (for PEDOT and PDTTs) or prepared by drop casting from tetrachloroethene solution (for PIM) on the surface of the reflection element. As the counter electrode, a Pt foil was used, as the quasi reference electrode, a Ag wire covered with AgCl. The potential of the electrode was determined as -350 mV vs. the ferrocene redox couple and turned out to be sufficiently stable throughout the experiment. Details of the setup are described in previous publications [15–17].

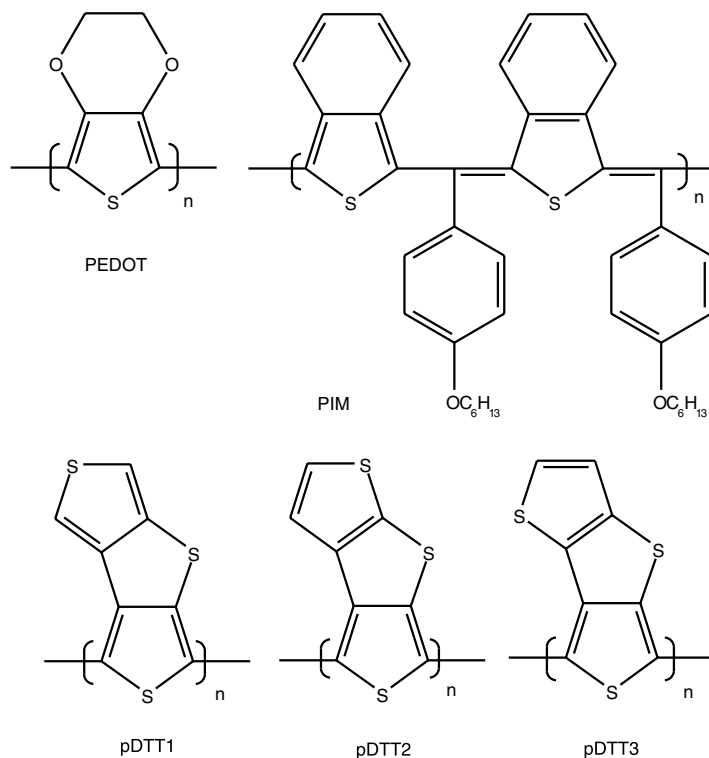


Fig. 1. Structures of the polymers.

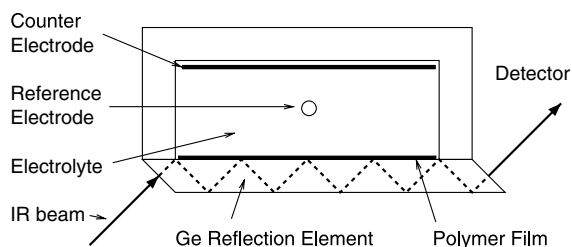


Fig. 2. Setup of the cell for ATR-FTIR spectroelectrochemistry.

Spectral changes were recorded consecutively during slow potential sweeps. To obtain specific spectral changes during individual electrochemical reaction processes, a spectrum just before the considered reaction is chosen as the reference spectrum. The subsequent spectra are related to that spectrum, showing only the spectral differences to the reference state. Each spectrum covers a range of about 90 mV in the cyclic voltammogram. As electrolyte solutions, 0.1 M solutions of tetraethylammoniumhexafluorophosphate (for p-doping of PEDOT), tetrabutylammoniumperchlorate (for PIM and for n-doping of PEDOT) and tetrabutylammoniumhexafluorophosphate (for PDTTs) in anhydrous acetonitrile were used.

3. Results and discussion

3.1. PEDOT

PEDOT combines high stability and high electrical conductivity in the doped form with a low optical band gap of approximately 1.6 eV [22]. As an antistatic material, PEDOT is already used industrially on a large scale [23]. Among electrically conducting polymers, PEDOT has one of the lowest oxidation potentials (onset of the oxidation peak in cyclic voltammograms at about -200 mV vs. Ag|AgCl [24]). Cyclic voltammetric results from n-doping of PEDOT films was first reported by Pei et al. [25].

In Fig. 3 the infrared spectra for the p-doping process and the n-doping process are compared (data taken from [18]). The spectra were obtained in situ during electrochemical oxidation and reduction processes and are rescaled to comparable band intensities (actually, the intensities of the bands during n-doping were smaller). Distinct differences are found: differences in relative band intensities, a band at 1513 cm^{-1} only in the p-doped form, new bands at 1285 and 1245 cm^{-1} only in the n-doped form, and a different maximum of the electronic absorption (4000 cm^{-1} for n-doping, 3000 cm^{-1} for p-doping).

Although a direct correlation to the calculated force field of polythiophene could not be obtained with n-doped PEDOT, the lower intensities of the IRAV bands

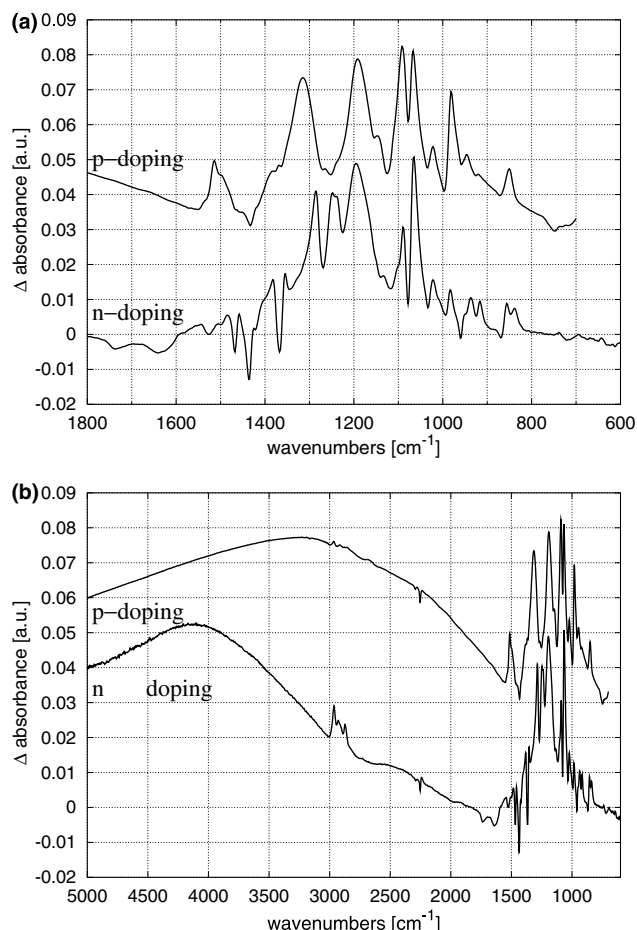


Fig. 3. In situ infrared spectra obtained during oxidation (p-doping, upper curves) and reduction (n-doping, lower curves) of PEDOT. The spectra are rescaled for similar band intensities. (a) IRAV range, (b) extended spectral range (data taken from [18]).

at a comparable doping level together with differences in the position and shape of the electronic absorption band and some IRAV bands indicate a higher localisation of the doping induced charge carriers and a smaller effective conjugation length in n-doped PEDOT [18].

3.2. PIM

A possible way to obtain low band gap materials is the realisation of alternating aromatic and quinoid thiophene units along the chain. Poly(heteroarylene methines) were presented by Jenekhe [26]. A soluble derivative of poly(isothianaphthene methine), PIM [27], shows good stability under ambient conditions and a band gap of about 1.5 eV [19]. In contrast to most other conjugated polymers, electrochemical doping of PIM shows two different consecutive p-doping processes and one process at n-doping.

Fig. 4 shows in situ infrared spectra for high p-doping, low p-doping and for n-doping (data taken from [19]). In the low p-doping regime, the IRAV

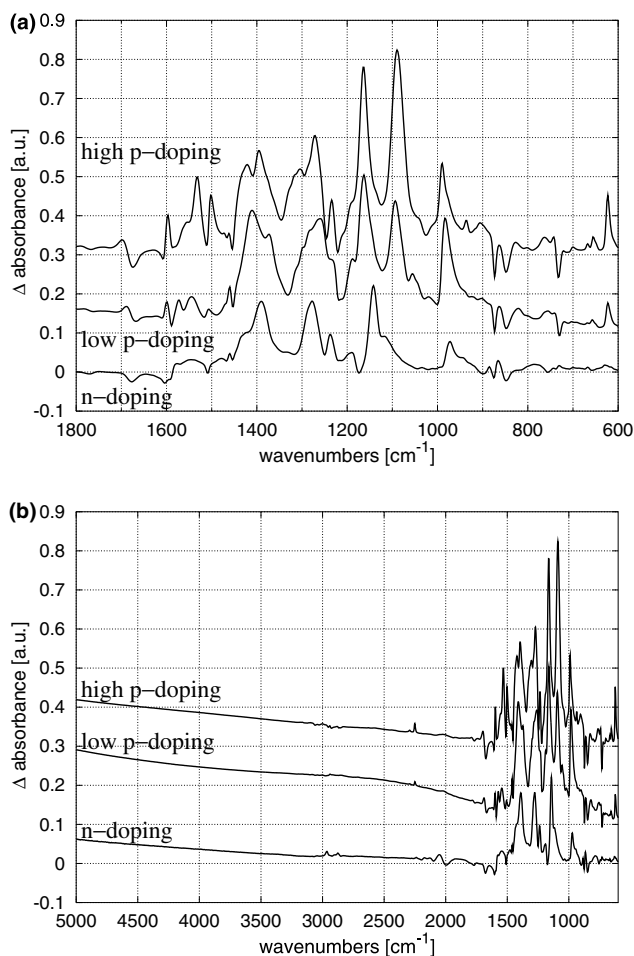


Fig. 4. In situ infrared spectra obtained during oxidation (high p-doping, upper curves; low p-doping, middle curves) and reduction (n-doping, lower curves) of PEDOT. The spectra are rescaled for similar band intensities. (a) IRAV range; (b) extended spectral range (data taken from [19]).

spectra show four strong IRAV bands around 1400, 1260–1280, 1165 and 985 cm^{-1} (the band around 1095 cm^{-1} is due to incorporated perchlorate counter ions). The similarity to the IRAV patterns obtained with substituted polythiophenes [4,28], where no quinoid chain segments are present, indicates that mostly aromatic units are involved in the low p-doping process. In the high p-doping regime additional IRAV bands especially in the region between 1500 and 1600 cm^{-1} appear, which can be attributed to C=C vibrations at either sides of the quinoid units [29]. The results show that mainly quinoid rings are affected by the high p-doping regime. The spectra obtained during n-doping are quite similar to the spectra of low p-doping. Again, mainly aromatic units are involved in the n-doping process.

The electronic absorption bands at higher energies (Fig. 4b) are rather weak. In addition, the intensities of the IRAV bands are quite low and remarkably sharp [19], indicating, that the delocalisation of the charges on

the chain is low. Structure calculations showed that the steric repulsion of the consequent polymer chain units results in a non-planar configuration [19]. Therefore, a low conjugation and a strong localisation of the charge carriers is obtained. PIM is a candidate for optical applications for low band gap materials but with an expected low charge carrier mobility.

3.3. PDTTs

PDTT1, PDTT2, and PDTT3 can be regarded as polythiophene-like chains in which a thienothiophene aromatic moiety is fused to each thiophene ring. Aromatic systems fused to thiophene rings increase the quinoidal character of the thiophene units and the π -electron delocalisation along the polymer chain [30,31], resulting in band gap values of 1.15 eV for PDTT1, 1.12 eV for pDTT2 and 1.05 eV for PDTT3 [32]. Despite the structural similarities, the different position of the sulfur atom in the outermost fused ring influences the aromaticity of the thiophene ring incorporated in the chain

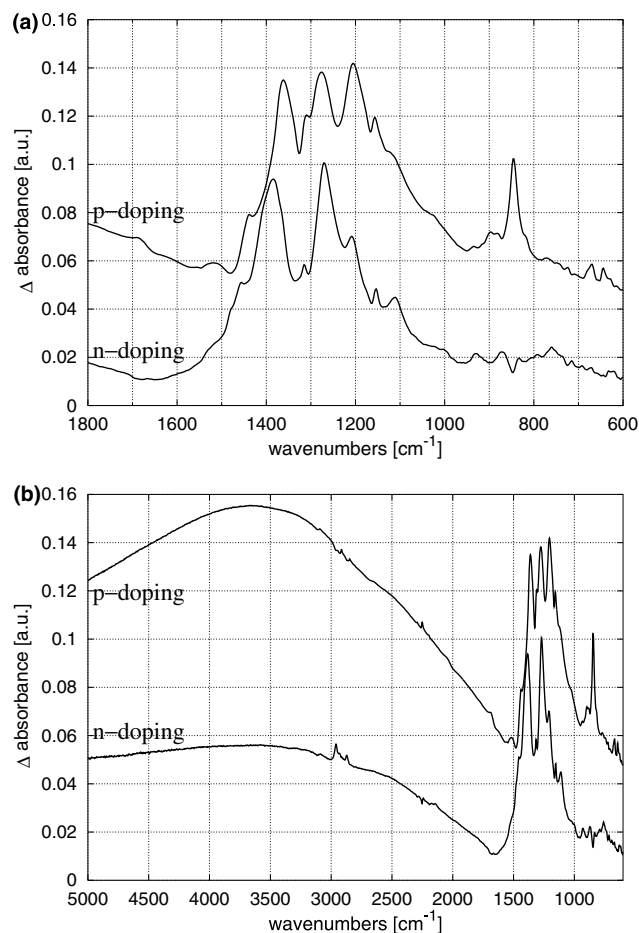


Fig. 5. In situ infrared spectra obtained during oxidation (p-doping, upper curves) and reduction (n-doping, lower curves) of PDTT1. The spectra are rescaled for similar band intensities. (a) IRAV range, (b) extended spectral range (data taken from [21]).

and therefore the electronic and the vibrational behaviour [21].

In Fig. 5 the in situ spectra for p-doping and n-doping of PDTT1 are compared (data taken from [21]). The sharp band at 842 cm^{-1} , growing during the p-doping of all PDTTs, is due to the incorporation of hexafluorophosphate ions balancing the charge formed on the polymer by the oxidation process. Differences between p- and n-doping of PDTT1 are found in the number of the main IRAV bands (three for p-doping, two for n-doping), in the frequency of the band maxima, and in the relative intensities of bands, particularly in the intensities of the electronic absorption bands (Fig. 5b).

Fig. 6 shows in situ spectra for p-doping and n-doping of PDTT2 (data taken from [21]). Again, a different spectral behaviour is obtained. The IRAV spectrum of the p-doped form is ill-defined due to the overlap of broad bands, while the n-doped polymer spectrum shows four distinct bands. In addition, the features below 800 cm^{-1} differ significantly.

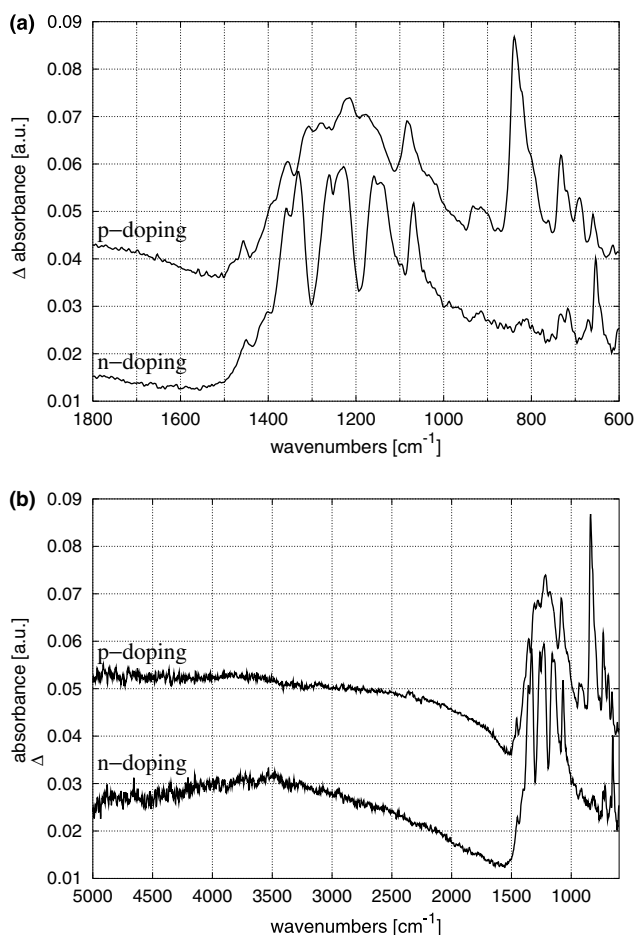


Fig. 6. In situ infrared spectra obtained during oxidation (p-doping, upper curves) and reduction (n-doping, lower curves) of PDTT2. The spectra are rescaled for similar band intensities. (a) IRAV range, (b) extended spectral range (data taken from [21]).

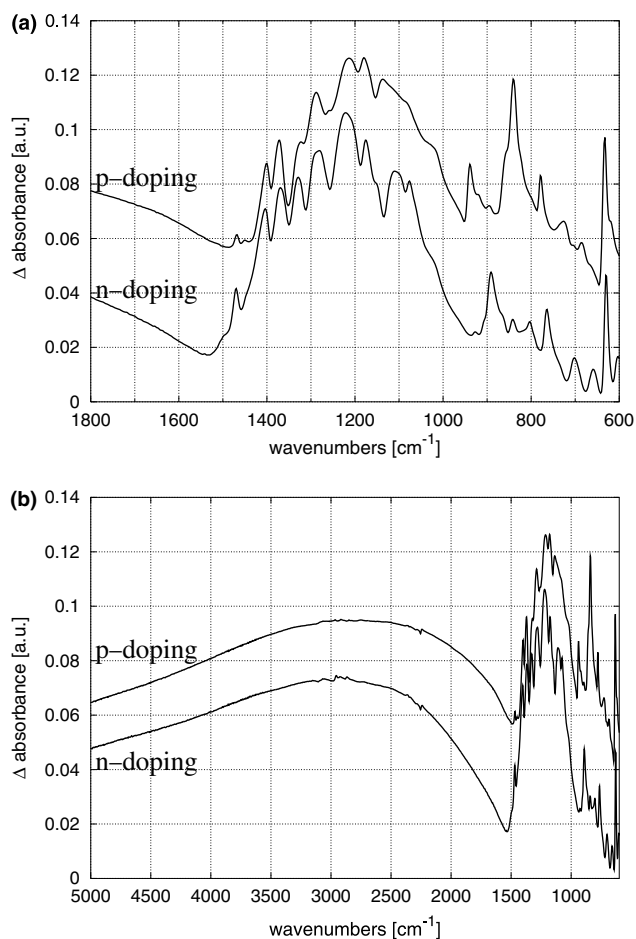


Fig. 7. In situ infrared spectra obtained during oxidation (p-doping, upper curves) and reduction (n-doping, lower curves) of PDTT3. The spectra are rescaled for similar band intensities. (a) IRAV range, (b) extended spectral range (data taken from [21]).

Similarly to the results observed with PEDOT, the IRAV bands of the n-doped forms of PDTT1 and PDTT2 are smaller than the p-doped forms of comparable doping level (for comparison, the spectra in Figs. 5–7 are rescaled to similar IRAV band intensities). Again, such differences together with smaller bandwidths and higher wavenumbers observed for the IRAV bands of the n-doped polymer forms [21] indicate a higher localisation of the negative charge carriers.

In contrast to PDTT1 and PDTT2, no substantial differences are found between the spectra of p- and n-doped PDTT3 (Fig. 7) [20], indicating rather similar structures and delocalisation extension for charge carriers of both signs. These properties may be interesting and favorable for certain optoelectronic devices and photovoltaic applications.

For all PDTTs, the doping induced IR spectra are quite different from the spectra obtained with simpler polythiophenes. The results show that the π -electrons of the fused thienothiophene moiety affect the π -electron delocalisation along the polythiophene-like chain. This

interaction is different for PDTT1, PDTT2 and PDTT3, resulting in a different spectral complexity and different electronic band gaps [21].

It should be noted, also that ESR spectroscopy shows different signals for p-doping and n-doping of PDTTs [21]. The spins of the positive carriers are found at g -factors higher than those reported for most p-doped conjugated polymers. The spin of negative carriers exhibits a shift of the g -factors to even higher values as compared to the positive polarons. However, a direct correlation of the shift of the g -values to differences in the doping behaviour was not obtained, since the similar shifts for all PDTTs do not reflect the different doping behaviour of PDTT1 and PDTT2 compared to PDTT3.

4. Conclusion

The doping induced infrared spectral behaviour of complex conjugated polymers turned out to be more complex than described by conventional theories, which were developed for systems such as polyacetylene and some simple polyheteroaromatics. These theories do not account for possible differences in the IRAV signatures of positive and negative charge carriers.

Studied with in situ infrared spectroelectrochemistry, the doping induced IRAV-bands for p- and n-doping (oxidation and reduction, respectively) of the thiophene based low band gap polymers PEDOT, PIM, PDTT1 and PDTT2 were found to be different, indicating that the materials exhibit different electronic structures with positive and negative charging. Mostly, the charge carriers are more localised in the case of n-doping. With PDTT3, similar spectra were obtained for p- and for n-doping, which indicates similar structures and delocalisation of the charges of both signs.

Due to the complexity of the polymer structures, the origin of the different charge localisation is still under discussion. Besides selective doping effects on different chain units (as for PIM) also charge trapping (which is probably more important for n-doping due to the usually high negative reduction potential) may contribute to the observed differences in the doping reactions.

An unusual electrochemical doping behaviour is shown by PIM, since it can be oxidised in two different processes (in contrast to most other conjugated polymers) to a low p-doped and a high p-doped form, and reduced in one process to the n-doped form. Interestingly, the IRAV pattern of the n-doped form and the low p-doped form are similar.

If extrapolated to other members of functionalised polythiophenes this finding may have important consequences for the design and performances of optoelectronic devices such as light emitting diodes and solar cells. Differences in the spectral features for p- and n-doping of conjugated polymers may also be used for the

identification of charge carriers formed either as primary excitations [33] or in a secondary process shortly after photoexcitation (e.g., via dissociation of excitons) [34,35] using fast time resolved spectroscopy.

Acknowledgements

The work was supported by the “Fonds zur Förderung der Wissenschaftlichen Forschung” (FWF) of Austria (P12680-CHE), and by the European Commission, RTN Project No. HPRN-CT-2000-00127 “EU-ROMAP”. The contribution of the coworkers Christoph Brabec, Marinella Catellani, Antonio Cravino, Lothar Dunsch, Ari Ivaska, Raf Kiebooms, Carita Kvarnström, Silvia Luzzati, Andreas Petr, N. Serdar Sariciftci, and Fred Wudl is gratefully acknowledged.

References

- [1] J. Orenstein, in: T.A. Skotheim (Ed.), Handbook of Conducting Polymers, Marcel Dekker, New York, 1986, Chapter 36.
- [2] B. Horowitz, Solid State Commun. 41 (1982) 729.
- [3] E. Ehrenfreund, Z.V. Vardeny, O. Brafman, B. Horowitz, Phys. Rev. B 36 (1987) 1535.
- [4] See for instance M. Del Zoppo, C. Castiglioni, P. Zuliani, G. Zerbi, in: T.A. Skotheim, R.L. Elsenbaumer, J.R. Reynolds (Eds.), Handbook of Conducting Polymers, second ed., Marcel Dekker, New York, 1988, Chapter 28 and references therein.
- [5] G. Zerbi, M. Gussoni, C. Castiglioni, in: J.L. Bredas, R. Silbey (Eds.), Conjugated Polymers, Kluwer Academic Publishers, Dordrecht, 1991, p. 435.
- [6] E. Ehrenfreund, Z.V. Vardeny, Proc. SPIE 324 (1997) 3145.
- [7] A. Girlando, A. Painelli, Z.G. Soos, J. Chem. Phys. 98 (1993) 7459.
- [8] F. Wudl, M. Kobayashi, A.J. Heeger, J. Org. Chem. 49 (1984) 3382.
- [9] J. Roncali, Chem. Rev. 97 (1997) 173.
- [10] C. Brabec, C. Winder, N.S. Sariciftci, J. Hummelen, A. Dhanaabalan, P. van Hal, R. Janssen, Adv. Funct. Mat. 12 (2002) 709.
- [11] S.E. Shaheen, C.J. Brabec, N.S. Sariciftci, F. Padinger, T. Fromherz, J.C. Hummelen, Appl. Phys. Lett. 78 (2001) 841.
- [12] A. Bewick, K. Kunitatsu, S.B. Pons, Electrochim. Act. 25 (1980) 465.
- [13] S.B. Pons, T. Davidson, A. Bewick, J. Electroanal. Chem. 125 (1981) 237.
- [14] A. Bewick, S. Pons, in: R.J. Clark, R.E. Hester (Eds.), Advances in Infrared and Raman Spectroscopy, vol. 12, Heyden & Son, London, 1985.
- [15] H. Neugebauer, N.S. Sariciftci, in: R.M. Metzger, P. Day, G.C. Papavassiliou (Eds.), Lower Dimensional Systems and Molecular Electronics, Nato ASI series, Series B: Physics, vol. 248, Plenum Press, New York, 1991, p. 401.
- [16] H. Neugebauer, Macromol. Symp. 94 (1995) 61.
- [17] C. Kvarnström, H. Neugebauer, A. Ivaska, in: H.S. Nalwa (Ed.), Advanced Functional Molecules and Polymers, vol. 2, Gordon & Breach Science Publishers, 2001, Chapter 3.
- [18] C. Kvarnström, H. Neugebauer, S. Blomquist, H.J. Ahonen, J. Kankare, A. Ivaska, N.S. Sariciftci, J. Mol. Struct. 521 (2000) 271.
- [19] H. Neugebauer, C. Kvarnström, C.J. Brabec, N.S. Sariciftci, R. Kiebooms, F. Wudl, S. Luzzati, J. Chem. Phys. 110 (1999) 12108.
- [20] A. Cravino, H. Neugebauer, S. Luzzati, M. Catellani, N.S. Sariciftci, J. Phys. Chem. B 105 (2001) 46.

- [21] A. Cravino, H. Neugebauer, S. Luzzati, M. Catellani, A. Petr, L. Dunsch, N.S. Sariciftci, *J. Phys. Chem. B* 106 (2002) 3583.
- [22] C. Gustafsson, B. Liedberg, O. Inganäs, *Solid State Ionics* 69 (1994) 145.
- [23] T. Cloots, F. Louwet, R. Andriessen, L. Bollens (AGFA Gevaert N.V.), Poster at the Symposium and Holst Memorial Lecture on Polymer Electronics, 1998.
- [24] C. Kvarnström, H. Neugebauer, S. Blomquist, H.J. Ahonen, J. Kankare, A. Ivaska, *Electrochim. Acta* 44 (1999) 2739.
- [25] Q. Pei, G. Zuccarello, M. Ahlskog, O. Inganäs, *Polymer* 35 (1994) 1347.
- [26] S.A. Jenekhe, *Nature* 322 (1986) 345.
- [27] R. Kiebooms, F. Wudl, *Synth. Met.* 101 (1999) 40.
- [28] G. Louarn, J.-Y. Mevellec, J.P. Buisson, S. Lefrant, *Synth. Met.* 55–57 (1993) 587.
- [29] G. Zerbi, M.C. Magnoni, I. Hoogmartens, R. Kiebooms, R. Carleer, D. Vanderzande, J. Gelan, *Adv. Mater.* 7 (1995) 1027.
- [30] J.L. Bredas, *Mol. Cryst. Liq. Cryst.* 49 (1985) 118.
- [31] O. Patil, A.J. Heeger, F. Wudl, *Chem. Rev.* 88 (1988) 183.
- [32] C. Arbizzani, M. Catellani, M. Mastragostino, M.G. Cerroni, *J. Electroanal. Chem.* 423 (1997) 23.
- [33] P.B. Miranda, D. Moses, A.J. Heeger, *Phys. Rev. B*, 64 (2001) 081201(R).
- [34] U. Mizrahi, E. Ehrenfreund, D. Gershoni, Z.V. Vardeny, *Synth. Met.* 119 (2001) 507.
- [35] U. Mizrahi, E. Ehrenfreund, D. Gershoni, Z.V. Vardeny, *Polymer* 44 (2003) 691.